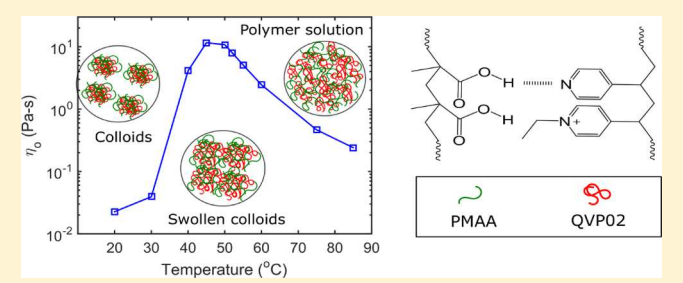
Thermothickening Behavior of Self-Stabilized Colloids Formed from Associating Polymers

Yaoyao Chen[©] and Kenneth R. Shull*[©]

Department of Materials Science and Engineering, Northwestern University, 2220 Campus Drive, Evanston, Illinois 60208, United States

Supporting Information

ABSTRACT: The complexation of partially ethyl-quaternized poly(4-vinyl pyridine) (QVP) and poly(methacrylic acid) (PMAA) induces a dramatic change in solution viscoelasticity. In this work, we investigated a model system consisting of QVP (with 2% charge), PMAA, and dimethyl sulfoxide (DMSO)—water mixed solvent (85 wt % DMSO—15 wt % water), which exhibits a remarkable thermothickening behavior, characterized by an increase of viscosity by 3 orders of magnitude when the temperature is increased by 20 °C. At low temperatures, this system behaves as a low-



viscosity milky colloidal suspension that remains stable for periods of at least 1 year. At higher temperatures, the colloids swell, increasing their effective volume fraction and giving rise to the observed viscosity increase. The thermothickening/thermothinning transition temperature could be tuned by varying the stoichiometry of the mixed polymers. We utilized rheometry, UV—vis spectroscopy, and dynamic light scattering to shed light on the mechanism of this phenomenon. This simple approach for achieving tunable thermothickening capability provides a new platform for designing thermoresponsive solutions from simple polymer mixtures.

INTRODUCTION

Thermoresponsive polymer solutions undergo structural transitions as a result of changes in the temperature, with marked changes in the resulting properties. This class of materials is useful for various applications including drug delivery, tissue engineering, energy storage,² and rheology modification in polymer processing.³ Depending on the nature of the thermal response, these polymer solutions fall into two categories: lower critical solution temperature (LCST) systems and upper critical solution temperature (UCST) systems. Most studies on thermoresponsive polymers in aqueous solution involve LCST systems, including poly(N-isopropylacrylamide) (PNIPAAm) and poly(propylene oxide) (PPO), enabling the critical temperatures to be tuned. The transition from a onephase state below the LCST to a two phase state above the LCST is an entropy-driven process, releasing solvent molecules from polymer aggregates to increase the entropy of the system. UCST systems, where the transition is enthalpy driven, are less common but are observed in systems with stronger polymer/ polymer or polymer/solvent interactions, often involving hydrogen bonding.4

Incorporation of more than one polymeric species is a particularly useful strategy for designing thermoresponsive polymers with more complex rheological properties. ^{5–7} Papagiannopoulos et al. reported that the introduction of a thermoresponsive moiety, PPO, to a bottle brush polymer leads to an unexpected temperature-thickening/temperature-thinning transition in aqueous solutions, corresponding to the conforma-

tional change from micellar structures to collapsed clusters with increasing temperature.⁵ Other types of amphiphilic architectures, for example, block copolymers, comb-shaped copolymers, and star-shaped polymers, have also been utilized.^{7–13}

In many applications of polymer solutions, the viscosity needs to be stabilized at a certain level over a wide range of temperatures. Most polymer solutions exhibit thermothinning behavior, with a temperature-dependent viscosity that can be described by an Arrhenius equation. To compensate the drop of viscosity due to temperature increase, thermothickening polymers are introduced to the system as viscosity modifiers. For example, various additives are added to drilling fluids for maintaining the viscosity level at high temperature. 14 PNIPAAm is the most frequently used thermosensitive moiety as grafting chains in thermothickening polymer systems, with the viscosity increasing by 3 orders of magnitude or more as the temperature is increased from 40 to 60 °C.15-17 There has been some investigation of thermothickening in mixtures of two homopolymers, 18 but a rich parameter space remains to be explored in these types of systems.

Our group recently reported a series of solvent-rich polymer complexes where one of the polymer species is partially quaternized poly(4-vinyl pyridine) (QVP). Polymer complexes in these systems are useful because of their

Received: May 13, 2019 Revised: June 6, 2019 Published: June 21, 2019

sensitivities to environmental conditions, such as ionic strength, pH, and solvent composition. ^{19–21} In the present work, we build on our previous understanding of these complexation mechanisms and explore their thermoresponsive behavior. We find that complexation of partially QVP and poly(methacrylic acid) (PMAA) induces a significant thermothickening/thermothinning transition. The multicomponent polymer solutions form stable colloidal suspensions at low temperatures that are stable for very long periods of time. An increase of temperature swells the QVP–PMAA complexes and softens the strength of the complexation simultaneously, resulting in an unusual thermal response (schematic in Figure 1). The

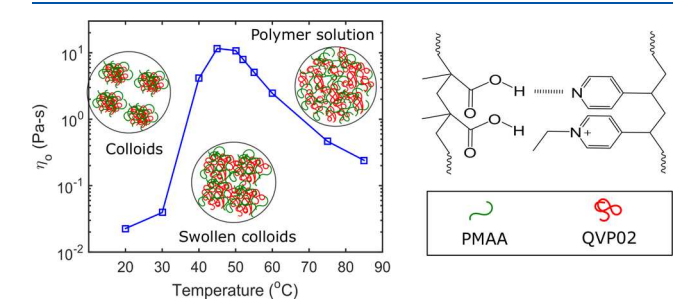


Figure 1. Schematic showing the design of thermoresponsive polymers based on the temperature-dependent formation of a self-stabilized emulsion from a mixture of associating polymers.

simplicity of polymer architecture and the controllability of polymer structures make this system a useful one for stabilizing suspensions while maintaining good processibility. At the same time, this new thermoresponsive mechanism inspires the design of thermoresponsive polymers and rheology modifiers from both scientific and application perspectives.

MATERIALS AND METHODS

Materials. Poly(4-vinyl pyridine) (P4VP, molecular weight, 200 kg/mol, Scientific Polymer Products Inc.) and PMAA (molecular weight, >100 kg/mol, Scientific Polymer Products Inc.) were used without further purification. Dimethyl sulfoxide (DMSO) was purchased from Sigma-Aldrich Company and used as received. Quaternization of P4VP was achieved by adding bromoethane (EtBr, Sigma-Aldrich, 98%) to a P4VP solution to reach the desired charge ratio. In our notation, QVP02 denotes partially quaternized P4VP with a charge fraction of 0.02. The chemical structures of P4VP and QVP02 were confirmed by ¹H NMR in a Bruker ADVANCE III, 500 MHz system, with spectra reported in our previous work. ¹⁹

Methods. Sample Preparation. Samples were prepared by mixing the desired amounts of QVP02, PMAA, and solvents (DMSO and water) in vials by constantly stirring the mixtures on a heating plate ($T \approx 65$ °C) to obtain transparent solutions, which were then removed from the hot plate and allowed to cool to room temperature. The solvent condition used in this work was fixed to be a mixed solvent containing 85 wt % DMSO and 15 wt % water. The total polymer concentration used was in the range of 1-12 wt %. We use wxx-AYY to represent a sample with a total polymer weight percentage of xx and a mole percentage of methacrylic acid of YY. The mole fraction here is defined as the percentage of methacrylic acid repeating units relative to the total of all polymer repeating units (methacrylic acid, quaternized vinylpyridine, and unquaternized vinylpyridine). Samples involved in this work are listed here:

 For the colloid packing and solution scaling study, samples with methacrylic acid mole fraction of 0.5 were used. These samples include w01-A50, w03-A50, w05-A50, w08-A50, w10-A50, and w12-A50. (2) For the investigations of the role of stoichiometry, the total polymer weight fraction was fixed at 8 wt %, varying the mole fraction of methacrylic acid across the full composition range. These samples include w08-A00 (pure QVP02), w08-A17, w08-A33, w08-A44, w08-A50, w08-A60, w08-A67, w08-A75, w08-A83, and w08-A100 (pure PMAA).

Turbidity. Turbidity measurements of polymer suspensions were conducted on a HP (Agilent) 8452 UV/Vis DAD spectrophotometer in the temperature range, 20–75 $^{\circ}\text{C}$. With constant stirring at the rate of 300 rpm, polymer solutions (3–10 wt %) were placed in plastic cells and the absorbance of light at wavelength of 400 nm was recorded at varied temperatures.

Dynamic Light Scattering. The sizes of aggregates in our suspensions were characterized by dynamic light scattering (DLS) utilizing a Zetasizer Nano ZS Malvern instrument, equipped with a He−Ne gas laser (633 nm wavelength). The detector was located at 173° scattering angle. Samples with an overall polymer concentration of 8 wt % were homogenized at ≈65 °C and cooled to room temperature. Prior to the measurements, they were diluted at room temperature to 1 wt % and then loaded in disposable solvent resistant microcuvettes. The reflective index of mixed solvent is 1.459, and the dielectric constant is 61.6, respectively. The details of the instrumentation could be found elsewhere. ²²

Rheology. Rheological properties of polymer solutions were probed by an Anton Paar 302 rheometer, using a cone-plate geometry (plate diameter, 50 mm; cone angle, 2°). To prevent solvent evaporation, a transparent plastic hood was used to seal the measuring system. Zero shear viscosities of samples were decided from flow tests at strain rates ranging from 0.01 to 100 s⁻¹.

RESULTS AND DISCUSSION

Rheology of Homogeneous Polymer Solutions at High Temperatures. To obtain homogeneous samples, all materials used in this study were first heated to temperature of \approx 65 °C so that the mixtures were in one-phase state, appearing as transparent solutions. At high temperatures, the *wxx*-A50 set of samples exhibit shear thinning at high shear rates. As an example, Figure 2 shows the flow behavior of w08-A50 sample at

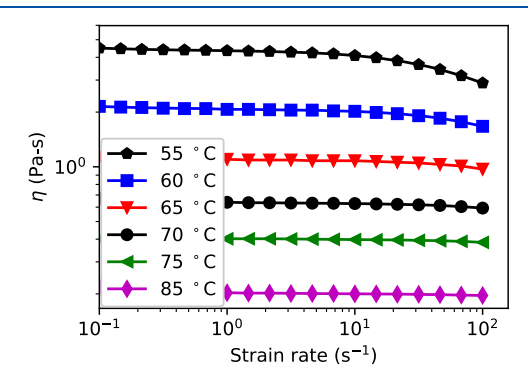


Figure 2. Strain rate dependence of viscosity for the w08-A50 sample in the high temperature regime (55–85 $^{\circ}$ C), where the polymer solution is homogeneous and transparent.

different temperatures (55–85 °C). These solutions possess a significant thermothinning behavior, as is demonstrated by the drop of viscosity at higher temperature. This is further illustrated in Figure 3, where relative viscosities, $\eta_{\rm r}$ obtained by dividing the zero-shear viscosities by the solvent viscosity (data shown in the Supporting Information) are plotted as a function of temperature for a series of solution concentrations. The following results are consistent with the behavior of associating polymer solutions driven by hydrogen bonding interactions between the unquaternized P4VP units and PMAA:

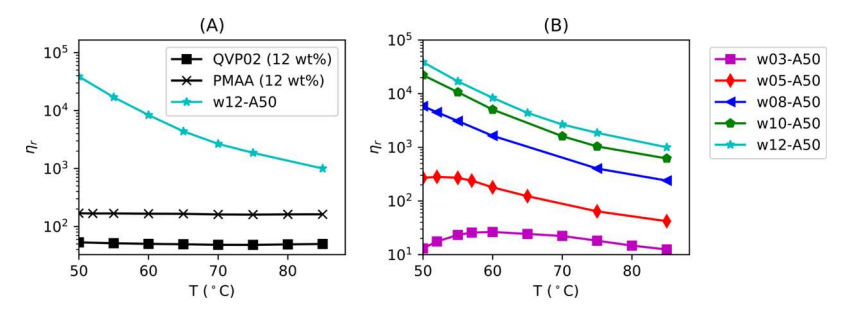


Figure 3. Temperature dependence of the relative viscosities of the polymer solutions in the high-temperature regime. (A) Comparison of PMAA, QVP02, and equimolar mixture of PMAA and QVP02, each at the total polymer concentration of 12 wt %. (B) Viscosities of a series of equimolar PMAA/QVP02 mixtures at different total polymer concentrations. In each case, the relative viscosity (η_r) is obtained by dividing the measured zero-shear viscosity (η_0) by the viscosity of the mixed solvent (15 wt % water–85 wt % DMSO) ($\eta_{solvent}$): $\eta_r = \eta_0/\eta_{solvent}$. Values for the temperature-dependent viscosities of this mixed solvent system are given in the Supporting Information. The measured mixed solvent viscosities were double-checked by comparing with values in similar conditions reported in ref 23.

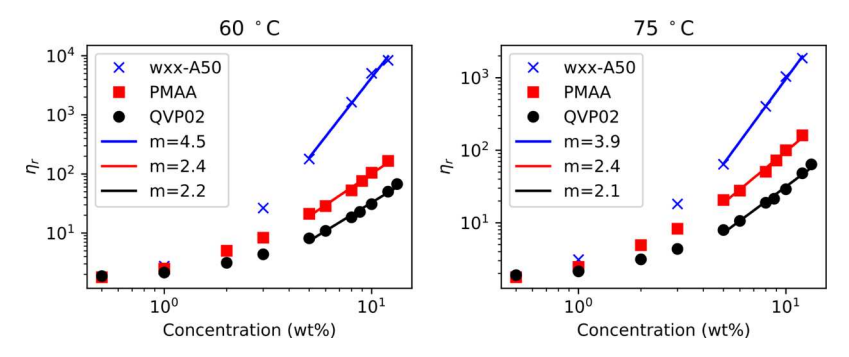


Figure 4. Concentration dependence of the relative viscosities of the component polymers and equimolar solutions of the two components at 60 and 75 °C. Power law exponents, *m*, describing concentration dependence at the higher concentrations are included and correspond to the sold lines.

- The viscosities of the polymer mixtures are substantially larger than the viscosities of either of the pure component polymers at the same concentrations (Figure 3A).
- The relative viscosities of the sufficiently concentrated solutions decrease with temperature (Figure 3B), with a temperature dependence determined by the nature of the hydrogen bonding interactions responsible for the viscosity enhancement.

The picture of this mixed polymer system is similar to Rubinstein's entangled dynamic associating polymer solution model,²⁴ where polymer chains form dynamic associations through secondary interactions, which in our case are hydrogen bonding interactions. Figure 4 describes the scaling of viscosities for mixed polymers and homopolymers, showing that mixed polymer solutions are much more viscous than homopolymer solutions at the same concentration. This behavior is direct evidence for the existence of interpolymer attractions that enhance the viscosity of the mixed polymer solutions. The mixing of proton-donating polymers, PMAA, and protonaccepting polymer, QVP02, causes the formation of dynamic associations, which can be viewed as attractive 'stickers' along the polymer chains. Power law exponents describing the concentration dependence of the different relative viscosities are shown in Figure 4, primarily to illustrate the fact that the difference between the mixed solution viscosity and the homopolymer solution viscosity increases both with increasing concentration and decreasing temperature.

To further evaluate the strength of the interactions responsible for determining the behavior of this system, we show Arrhenius plots of the relative viscosities in Figure 5. The slope of $\log(\eta_r)$ versus 1/T is an indicator of the apparent

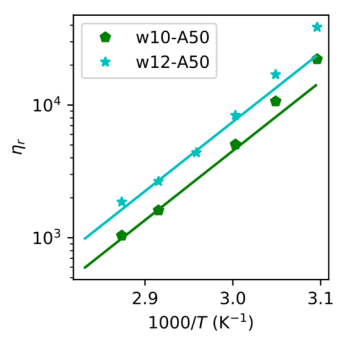


Figure 5. Arrhenius plots for the stoichiometrically balanced samples. The solid lines correspond to an activation energy of 100 kJ/mol.

activation energy. It should be noted that we only use a narrow temperature range (50–80 $^{\circ}$ C) for the fitting, and so, Arrhenius equation only gives an approximation on the association energy level, which is \sim 100 kJ/mol, comparable to the reported values with similar associating structures. ^{15,25–28}

Phase Behavior and Suspension Characterization at Low Temperatures. At temperatures below ~50 °C, the mixed polymer system becomes a stable milky suspension. This behavior mimics the behavior of the QVP polymer, the solubility of which depends on the degree of charge, solvent composition, and temperature. Our chosen solvent composition (85 wt % DMSO-15 wt % water) is not a good solvent for QVP02 at room temperature, resulting in inhomogeneous polymer clusters when the polymer concentration is 8 wt %. Increasing the temperature enhances the solubility of QVP02, giving a transparent polymer solution when the system is heated to ~50 °C. The incorporation of a second polymer, PMAA (which

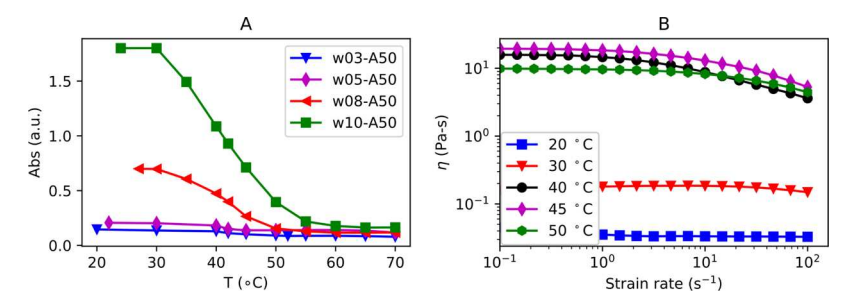


Figure 6. (A) Turbidity measurements for stoichiometrically balanced samples at different solution concentrations (wxx-A50). (B) Strain rate dependence of viscosity for the w08-A50 sample in the low temperature regime (\leq 50 °C).

is soluble at all temperatures used in our investigation), yields a milky suspension when the solution is cooled to room temperature. This suspension remains stable at room temperature for at least 1 year. When heated to $\sim 50\,^{\circ}$ C, the suspension reversibly transitions to a more transparent solution, which scatters less light as is demonstrated in Figure 6A.

In the appropriate concentration regime, the colloidal suspensions formed at low temperatures have much lower viscosities than the homogeneous solutions that exist at higher temperatures. These suspensions remain macroscopically homogeneous, behaving as Newtonian liquids or viscoelastic liquids with slight shear thinning behavior (in Figure 6B). The viscosities of these suspensions are affected dramatically by the temperature. For w08-A50, viscosity value increases from 0.02 to 10 Pa·s as the temperature is increased from 20 to 50 °C. This solution remains transparent at higher temperatures and the viscosity decreases from its maximum value by a factor of about 50 as the temperature is increased to 85 °C, as is discussed in previous section (see Figure 3B).

Hydrogen bonding is the attractive interaction that drives the complexation of QVP02 and PMAA, forming insoluble colloids at room temperature. The soluble component, PMAA, is the hydrogen bonding donor for the association of QVP02 and PMAA. PMAA presumably acts as a surfactant for stabilizing colloids because PMAA favors both QVP02 and the solvent. An increase in temperature weakens the QVP02–PMAA interactions, swelling the colloids and increasing their overall volume fraction in the suspension. This swelling is responsible for the observed thermothickening behavior.

An open question concerns the role of the small degree of charge in stabilizing the emulsions. We know from previous work on the roles of solvent composition and charge density that the charge enhances the one phase region where homogeneous solutions are obtained. We also observed in this previous work that the viscosity in the one-phase region is strongly dependent on the charge fraction of the QVP, much more than that would be expected just from a simple dilution of the proton accepting vinylpyridine groups. Presumably one effect of the charge is to mediate the ability of hydrogen bonds to form in this system. A more direct role in stabilizing the dispersion by providing an additional stabilization mechanism directly related to the incorporation of the charge cannot be ruled out entirely, however.

Figure 7 gives the correlations between viscosity and temperature for wxx-A50 samples in the full temperature range, 20–85 °C. All of these mixtures follow the trend of thermothickening/thermothinning transition, with a maximum in the viscosity observed between 45 and 60 °C, with the specific value of this temperature decreasing with increasing polymer concentration. The key finding we want to emphasize is the well-

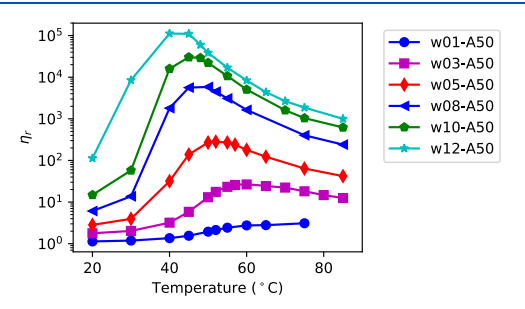


Figure 7. Full temperature dependence of the stoichiometrically balanced solution viscosity at different concentrations.

defined thermoresponsive behavior across in the polymer concentration range. This maximum in the viscosity as a function of temperature is rarely observed in polymer solutions. To achieve the combined effect of thickening and thinning in one single system, more complicated architectures (e.g., bottlebrush, block copolymers) are typically needed. To the best of our knowledge, the conventional mixing of QVP02 and PMAA reported in this work is the simplest method for producing polymer suspensions with this type of thermal response.

Effects of Stoichiometry. In traditional colloidal suspensions, additional surfactants are often added in order to introduce repulsive interactions between individual particles. 30-32 In our case, the colloids are presumably stabilized by a PMAA-rich layer that forms at the particle/solution interface. To gain a better understanding of the factors that enable these self-stabilized emulsions to form, we investigated a series of nonstoichiometric polymer suspensions at a fixed polymer weight fraction of 8 wt %. Figure 8 shows the effect of stoichiometry on the rheological behavior of this system. Images of the samples are shown in Figure 9A, and we compare the composition dependence of the relative viscosity at 20 and 70 $^{\circ}$ C in Figure 9B. This comparison of η_r at 20 and 70 °C gives a description of the conditions for which thermothickening is observed, with thermothic kening behavior observed for $X_{\rm MAA}$ < 0.55 where η_r at 70 °C exceeds the value of η_r at 20 °C.

At room temperature, the QVP02 polymer does not form a macroscopically homogeneous suspension but instead appears as a collection of solvent-swollen precipitates that can be emulsified by the inclusion of PMAA. The addition of 17% PMAA to QVP02 is sufficient to enable the formation of a stable, opaque suspension (Figure 9A). Further increases of the PMAA content reduce the hydrodynamic diameter of the polymer rich suspension droplets from 330 to 138 nm, as shown by the DLS results in Table 1 and Figure 10. The specific particle size is controlled at least partially by kinetic factors and is influenced by the detailed processing scheme. For example, if the 1% solution formed from dilution of the w08-A50 sample is reheated and

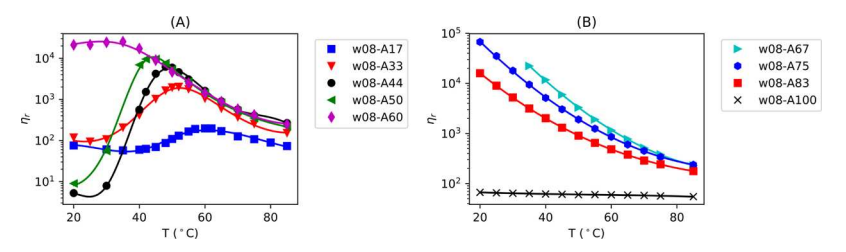


Figure 8. Temperature dependence of relative viscosities for samples with different stoichiometries, each with an overall polymer concentration of 8 wt %. Samples with lower PMAA fractions (\leq 60%) are shown in (A) and those with higher PMAA fractions (\geq 67%) are shown in (B).

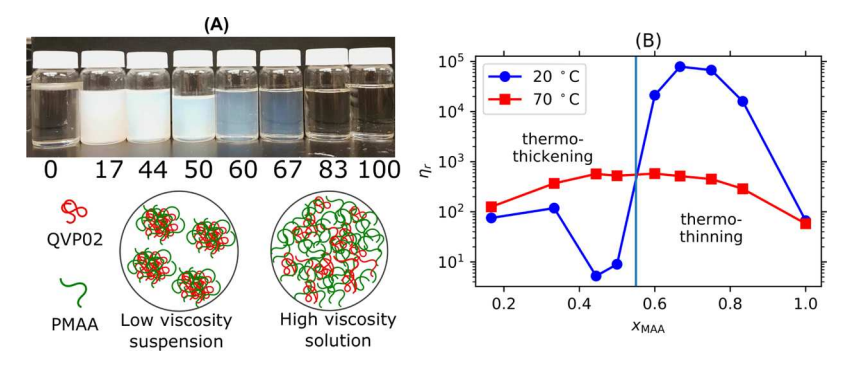


Figure 9. Influence of stoichiometry on the properties of a series of samples, each having an overall polymer concentration of 8 wt %. Images are shown in (A) with the numbers corresponding to the mole percentages of PMAA in the polymer mixture. Viscosities at 20 and 70 $^{\circ}$ C as functions of PMAA molar fraction are plotted in (B).

Table 1. Sizes and Polymer Concentrations of the w08-AYY Colloids as Determined in a Series of Different Samples at 20 $^{\circ}$ C^a

sample	temperature (°C)	diameter (nm)	standard error (nm)	φ*c _d (wt %)	$(\phi^* = 0.75)$ (wt %)
w08-A17	20	330	73	9.04	12.0
w08-A33	20	166	36	8.81	11.7
w08-A44	20	151	45	14.2	18.9
w08-A50	20	147	30	13.3	17.7
w08-A60	20	138	27		
w08-A50	30			11.7	15.6

"The sizes were determined by DLS and the polymer concentrations within the colloids, (c_d) , were obtained by forcing agreement of the measured values of the viscosity at c = 8 wt % to the predictions of eq 3, with $\phi^* = 0.75$.

cooled back to room temperature, the hydrodynamic diameter of the particles is reduced from 147 to 120 nm. Dilution or long-term storage of the samples at room temperature, however, does not lead to any measurable change in the size of the colloids

obtained during the cooling process. Clear solutions are obtained when the PMAA mole fraction exceeds 0.83.

Figure 11 gives an overall picture of the temperature and composition dependence of the viscosity response for systems with an overall polymer concentration of 8 wt %. The diameters of the symbols scale with the magnitude of $d[\log(\eta_r(T))]/dT$, obtained from the fits represented by the solid lines in Figure 8. Red symbols correspond to thermothickening behavior where the viscosity increases with temperature, and blue symbols correspond to thermothinning behavior where the viscosity decreases with increasing temperature. The boundary between the thermothickening and thermothinning regimes corresponds to the viscosity maximum, represented by the solid line in Figure 11. This transition temperature decreases as the PMAA content increases and correlates very well with the cloud points obtained from the absorbance measurements. These cloud points are represented by the dashed line in Figure 11, and are defined as the temperature at which the absorbance of the solution is halfway between the limiting values obtained at high and low temperatures. The detailed procedure for obtaining these cloud points is described in the Supporting Information. It is clear

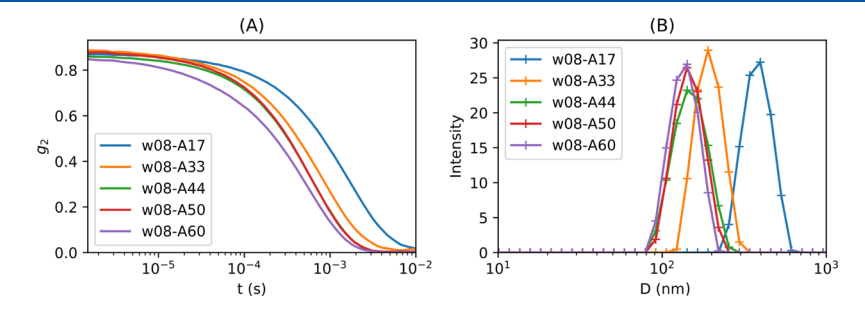


Figure 10. (A) Correlation functions of different samples [w08-AYY (YY = 17, 33, 44, 50, and 60)] in DLS measurements at temperature 20 °C. Measurements were performed at the polymer concentration of 1 wt %, obtained by room temperature dilution of w08-AYY. (B) Size distributions of colloidal particles obtained from different samples.

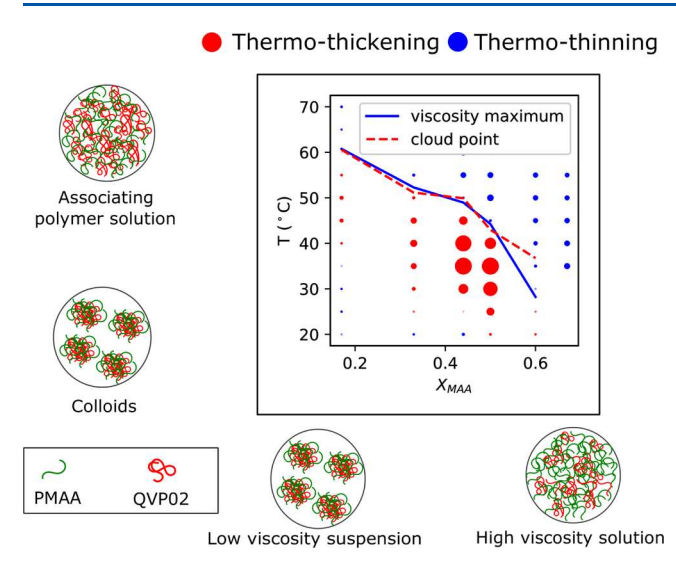


Figure 11. Overall picture of the QVP02—PMAA system at an overall polymer concentration of 8 wt %. $X_{\rm MAA}$ is the mole fraction of PMAA within mixed polymers. The diameters of the symbols scale with ${\rm d}[\log(\eta_{\rm r}(T))]/{\rm d}T$, with positive values of this quantity in red and negative values in blue. Viscosity values correspond to the data in Figure 8. Cloud points were taken from the turbidity measurements (detailed results in the Supporting Information) and correspond closely to the temperature at which the viscosity is maximized.

from Figure 11 that the maximum thermothickening response is obtained for nearly stoichiometric solutions at temperatures just below the onset of phase separation into a stabilized suspension.

Colloidal Packing Model. As discussed above, the behavior of this system at high temperatures is not unusual for high molecular polymer solutions with associating groups. The unique signature of this system is the phase separation at lower temperatures to regions of high and low polymer concentrations. The more highly concentrated regions of the materials segregate into a stabilized, sub-micrometer dispersed phase that is highly resistant to subsequent coalescence. We can obtain an estimation for the polymer concentration in the dispersed phase by utilizing well-established models for the viscosity of colloidal dispersions. A variety of models have been utilized, but the following simple functional form is suitable for our purposes^{33–36}

$$\eta_{\rm r} = [1 - \phi/\phi^*]^{-2} \tag{1}$$

Here ϕ is the volume fraction of the colloidal phase and ϕ^* is a critical packing volume fraction. Bicerano et al. have suggested some corrections to eq 1,37,38 which account for the particle rigidity, particle/particle interactions, and so forth. However, these corrections are generally quite small and are not necessary here, where we desire a simple and reasonably accurate expression relating the particle volume fraction to the measured viscosity. Considering that the sizes of particles are in the order of ~100 nm and the contribution of Brownian force is nonnegligible, the flow behavior of these suspensions in our study is more complicated compared with Newtonian liquids. Shikata and Pearson gave a comprehensive analysis of shear rate dependence of concentrated spherical particle suspensions in this regime, suggesting that eq 1 might still work for this situation although ϕ^* needs to be adjusted correspondingly.^{39,40} In our own case, we are seeking for a relatively simple expression that could be used for fitting our viscosity data and revealing the packing details. Thus, we only utilize this simple form without further discussing Brownian forces. The sufficiency of eq 1 for this purpose is illustrated by Figure 12, where we plot measured

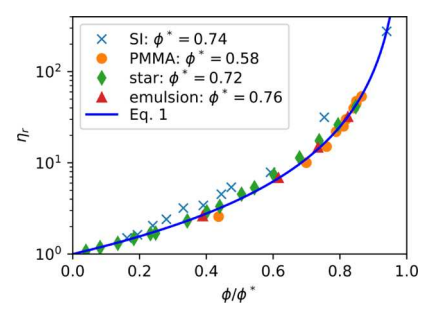


Figure 12. Literature data for the reduced viscosity as a function of the normalized reduced volume fraction of the dispersed phase. Values of ϕ^* used for the normalization in each case are shown in the legend. Data are included for styrene/isoprene block copolymer micelles (SI, sample SI-600 from ref 35), poly(methyl methacrylate) (PMMA, 640 nm sample from ref 35), a highly branched star molecule (star, sample 12 880 from ref 35), and an emulsion with a viscosity ratio for the dispersed and continuous phases of ≈ 1000 (emulsion, from ref 40). The solid line is a representation of eq 1.

values of the relative viscosity against the particle volume fraction for a range of systems, comparing to eq 1, with ϕ^* treated as an adjustable parameter. Data from the literature are included for dispersed poly(methyl methacrylate) spheres,³⁵ styrene isoprene block copolymer micelles with polystyrene cores and polyisoprene corona block, providing steric stabilization,³⁵ a compact star-branched copolymer³⁵ and an emulsion with a viscosity ratio of ≈1000 between the dispersed and continuous phases. 41 For each of these situations, eq 1 provides an adequate description of the concentration dependence of the relative viscosity, although this is no longer the case for less compact star-branched polymers, which begin to behave as polymer solutions but not as colloidal suspensions.³⁵ The emulsion data are most relevant to our case because our situation is similar, although with a much larger value of the viscosity ratio. A value of ≈ 0.75 for ϕ^* is a representative of the soft, deformable systems shown in Figure 12, and we use this value in our analysis.

By assuming that all of the polymers exist in the colloidal particle phase and the medium only consists of solvent, we obtain the following for ϕ

$$\phi = c/c_{\rm d} \tag{2}$$

where c is the overall weight fraction of polymer in the system and c_d is the weight fraction of polymer within the colloidal particles. With this definition of ϕ , we can rewrite eq 1 in the following form:

$$\eta_{\rm r} = \left[1 - \frac{c}{\phi^* c_{\rm d}}\right]^{-2} \tag{3}$$

Figure 13 demonstrates the effectiveness of eq 3 in describing the concentration dependence of the viscosity of our systems at low temperatures. We obtain ϕ^*c_d = 13.3 wt % at 20 °C and ϕ^*c_d = 11.7 wt % at 30 °C. By choosing a value of 0.75 for ϕ^* (consistent with the behavior of the soft colloids in Figure 12), we obtain c_d = 17.7 wt % at 20 °C and c_d = 15.6 wt % at 30 °C. The situation is more complicated at 40 °C, where the picture of isolated non-interacting colloids is not a suitable representation of the behavior of the system.

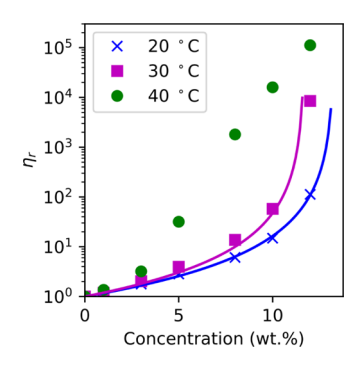


Figure 13. Relative viscosity for stoichiometric samples at relatively low temperatures (\leq 40 °C). The solid lines are representations of eq 3, with $\phi^*c_d = 13.3$ wt % at 20 °C and $\phi^*c_d = 11.7$ wt % at 30 °C.

We further use the measured values of η_r in w08-AYY (Figure 8) in conjunction with eq 3 to estimate the value of ϕ^*c_d for each suspension at 20 °C. Again, assuming a value of 0.75 for the critical packing fraction, ϕ^* , we obtain the estimates for c_d , the polymer concentration within the suspended, polymer-rich phase, listed in Table 1. The colloidal particle phase is most concentrated for systems that have the same mole concentration of two polymers or have a slight excess of QVP02 relative to MAA ($X_{\text{MAA}} = 0.44$ and $X_{\text{MAA}} = 0.5$). In these systems, the polymer concentration in colloidal particles (12-19 wt %) is approximately twice as large as the average polymer concentration in the mixture (8 wt %), giving value for the effective polymer volume fraction, ϕ of ~0.5, which is substantially less than the critical packing fraction, ϕ^* . As the suspension is heated, the value of c_d decreases, increasing ϕ and giving a rapid increase in the viscosity as ϕ approaches ϕ^* . When ϕ exceeds ϕ^* , eq 3 can no longer be used. In this case, the suspension property transitions to one-phase homopolymer solution, the viscosity of which is much higher than that of the low temperature suspension, with details discussed in previous sections.

CONCLUSIONS

In this work, we performed extensive experimental study of multicomponent associating polymer solutions, made from mixtures of PMAA and QVP02, in a solvent consisting of 85 wt % DMSO and 15 wt % water. Clear, one-phase solutions are obtained above an UCST that ranges from 45 to 60 °C, depending on detailed composition of the polymer mixture. Above this temperature, the system behaves as an associating polymer solution, with a viscosity that is much larger than the viscosity of either of the component polymers at the same overall polymer concentration. Below this critical temperature, the solution forms a colloidal suspension of more concentrated submicron polymer droplets, with polymer concentration within the droplets ranging from 12 to 19 wt %, depending on the temperature and relative amounts of QVP02 and PMAA in the system. This droplet phase is stabilized against coalescence, and this suspension has a much lower viscosity than the associating polymer solution formed at higher temperatures. As a result of this behavior, it is possible to design solutions for which the viscosity increases by a factor of 1000 as the temperature is increased by 20 °C. The behavior is controlled by the hydrogen bonding interactions between acid and pyridine groups, which are mediated by the small amount of charge (2% of the pyridine moieties) introduced by the partial quaternization. This work paves the way for designing thermoresponsive polymers

solutions that are quite easy to formulate and yet exhibit a range of temperature-dependent properties.

ASSOCIATED CONTENT

Supporting Information

The Supporting Information is available free of charge on the ACS Publications website at DOI: 10.1021/acs.macromol.9b00973.

Viscosities of mixed solvents, UV-vis absorbance, and sample images (PDF)

AUTHOR INFORMATION

Corresponding Author

*E-mail: k-shull@northwestern.edu.

ORCID ®

Yaoyao Chen: 0000-0002-9217-5769 Kenneth R. Shull: 0000-0002-8027-900X

Notes

The authors declare no competing financial interest.

ACKNOWLEDGMENTS

The authors acknowledge financial supports from the National Science Foundation (DMR-1710491), the 3M Graduate Fellowship program, and the Center for Hierarchical Materials Design (CHiMaD). This work made use of the MatCI Facility which receives support from the MRSEC Program (NSF DMR-1720139) of the Materials Research Center at Northwestern University and the IMSERC facility, which has received support from the Soft and Hybrid Nanotechnology Experimental (SHyNE) Resource (NSF NNCI-1542205), the State of Illinois and the International Institute for Nanotechnology. The authors also want to thank Prof. Derk Joester for providing the DLS instrument for particle size measurements.

REFERENCES

- (1) Ward, M. A.; Georgiou, T. K. Thermoresponsive Polymers for Biomedical Applications. *Polymers* **2011**, *3*, 1215–1242.
- (2) Shen, J.; Han, K.; Martin, E. J.; Wu, Y. Y.; Kung, M. C.; Hayner, C. M.; Shull, K. R.; Kung, H. H. Upper-critical solution temperature (UCST) polymer functionalized graphene oxide as thermally responsive ion permeable membrane for energy storage devices. *J. Mater. Chem. A* **2014**, *2*, 18204–18207.
- (3) Lee, Y. R.; Park, D.; Choi, S. K.; Kim, M.; Baek, H. S.; Nam, J.; Chung, C. B.; Osuji, C. O.; Kim, J. W. Smart Cellulose Nanofluids Produced by Tunable Hydrophobic Association of Polymer-Grafted Cellulose Nanocrystals. *ACS Appl. Mater. Interfaces* **2017**, *9*, 31095—31101.
- (4) Seuring, J.; Agarwal, S. Polymers with Upper Critical Solution Temperature in Aqueous Solution: Unexpected Properties from Known Building Blocks. *ACS Macro Lett.* **2013**, *2*, 597–600.
- (5) Papagiannopoulos, A.; Zhao, J.; Zhang, G.; Pispas, S.; Jafta, C. J. Viscosity Transitions Driven by Thermoresponsive Self-Assembly in PHOS- *g* -P(PO- *r* -EO) Brush Copolymer. *Macromolecules* **2018**, *51*, 1644–1653.
- (6) Marić, M.; Zhang, C.; Gromadzki, D. Poly(methacrylic acid-ran-2-vinylpyridine) Statistical Copolymer and Derived Dual pH-Temperature Responsive Block Copolymers by Nitroxide-Mediated Polymerization. *Processes* **2017**, *5*, 7.
- (7) Ren, H.; Chen, D.; Shi, Y.; Yu, H.; Fu, Z.; Yang, W. Charged End-Group Terminated Poly(N-isopropylacrylamide)-b-poly(carboxylic azo) with Unusual Thermoresponsive Behaviors. *Macromolecules* **2018**, *51*, 3290–3298.
- (8) Bossard, F.; Tsitsilianis, C.; Yannopoulos, S. N.; Petekidis, G.; Sfika, V. A Novel Thermothickening Phenomenon Exhibited by a

Triblock Polyampholyte in Aqueous Salt-Free Solutions. *Macromolecules* **2005**, *38*, 2883–2888.

- (9) Wu, G.; Chen, S.-C.; Zhan, Q.; Wang, Y.-Z. Well-Defined Amphiphilic Biodegradable Comb-Like Graft Copolymers: Their Unique Architecture-Determined LCST and UCST Thermoresponsivity. *Macromolecules* **2011**, *44*, 999–1008.
- (10) Mishra, V.; Jung, S.-H.; Jeong, H. M.; Lee, H.-i. Thermoresponsive ureido-derivatized polymers: the effect of quaternization on UCST properties. *Polym. Chem.* **2014**, *5*, 2411.
- (11) Yuan, W.; Chen, X. Star-shaped and star-block polymers with a porphyrin core: from LCST-UCST thermoresponsive transition to tunable self-assembly behaviour and fluorescence performance. RSC Adv. 2016, 6, 6802–6810.
- (12) Palanisamy, A.; Sukhishvili, S. A. Swelling Transitions in Layer-by-Layer Assemblies of UCST Block Copolymer Micelles. *Macromolecules* **2018**, *51*, 3467–3476.
- (13) Shangguan, Y.; Liu, M.; Jin, L.; Wang, M.; Wang, Z.; Wu, Q.; Zheng, Q. Thermo-thickening behavior and its mechanism in a chitosan-graft-polyacrylamide aqueous solution. *Soft Matter* **2018**, *14*, 6667–6677.
- (14) Xie, B.; Liu, X. Thermo-thickening behavior of LCST-based copolymer viscosifier for water-based drilling fluids. *J. Pet. Sci. Eng.* **2017**, *154*, 244–251.
- (15) Annable, T.; Buscall, R.; Ettelaie, R.; Whittlestone, D. The rheology of solutions of associating polymers: Comparison of experimental behavior with transient network theory. *J. Rheol.* **1993**, 37. 695–726.
- (16) Díaz-Silvestre, S. E.; St Thomas, C.; Rivera-Vallejo, C.; Cadenas-Pliego, G.; Pérez-Alvarez, M.; de León-Gómez, R. D.; Jiménez-Regalado, E. J. Concentration effect of N-isopropylacrylamide on viscoelastic properties of hydrosoluble thermo-thickening copolymers. *Polym. Bull.* **2017**, *74*, 4009–4021.
- (17) Vasile, C.; Bumbu, G.-G.; Mylonas, I.; Bokias, G.; Staikos, G. Thermoresponsive behaviour in aqueous solution of poly(maleic acidalt-vinyl acetate) grafted with poly(N-isopropylacrylamide). *Polym. Int.* **2004**, 53, 1176–1179.
- (18) de Lima, B. V.; Vidal, R. R. L.; do N Marques, N.; S Maia, A. M.; de C Balaban, R. Temperature-induced thickening of sodium carboxymethylcellulose and poly(N-isopropylacrylamide) physical blends in aqueous solution. *Polym. Bull.* **2012**, *69*, 1093–1101.
- (19) Chen, Y.; Shull, K. R. High-Toughness Polycation Cross-Linked Triblock Copolymer Hydrogels. *Macromolecules* **2017**, *50*, 3637–3646.
- (20) Mathis, L.; Chen, Y.; Shull, K. R. Tuning the Viscoelasticity of Hydrogen-Bonded Polymeric Materials through Solvent Composition. *Macromolecules* **2018**, *51*, 3975–3982.
- (21) Sadman, K.; Wang, Q.; Chen, Y.; Keshavarz, B.; Jiang, Z.; Shull, K. R. Influence of Hydrophobicity on Polyelectrolyte Complexation. *Macromolecules* **2017**, *50*, 9417–9426.
- (22) Liaw, C. Y.; Henderson, K. J.; Burghardt, W. R.; Wang, J.; Shull, K. R. Micellar Morphologies of Block Copolymer Solutions near the Sphere/Cylinder Transition. *Macromolecules* **2015**, *48*, 173–183.
- (23) del Carmen Grande, M.; Juliá, J. A.; García, M.; Marschoff, C. M. On the density and viscosity of (water+dimethylsulphoxide) binary mixtures. *J. Chem. Thermodyn.* **2007**, *39*, 1049–1056.
- (24) Rubinstein, M.; Semenov, A. N. Dynamics of Entangled Solutions of Associating Polymers. *Macromolecules* **2001**, *34*, 1058–1068
- (25) Séréro, Y.; Aznar, R.; Porte, G.; Berret, J.-F.; Calvet, D.; Collet, A.; Viguier, M. Associating polymers: from "flowers" to transient networks. *Phys. Rev. Lett.* **1998**, *81*, 5584.
- (26) Séréro, Y.; Jacobsen, V.; Berret, J.-F.; May, R. Evidence of Nonlinear Chain Stretching in the Rheology of Transient Networks. *Macromolecules* **2000**, 33, 1841–1847.
- (27) Robin, C.; Lorthioir, C.; Amiel, C.; Fall, A.; Ovarlez, G.; Le Cœur, C. Unexpected Rheological Behavior of Concentrated Poly-(methacrylic acid) Aqueous Solutions. *Macromolecules* **2017**, *50*, 700–710.

- (28) Wang, J.; Benyahia, L.; Chassenieux, C.; Tassin, J.-F.; Nicolai, T. Shear-induced gelation of associative polyelectrolytes. *Polymer* **2010**, *51*, 1964–1971.
- (29) Zhunuspayev, D. E.; Mun, G. A.; Hole, P.; Khutoryanskiy, V. V. Solvent Effects on the Formation of Nanoparticles and Multilayered Coatings Based on Hydrogen-Bonded Interpolymer Complexes of Poly(acrylic acid) with Homo- and Copolymers of *N*-Vinyl Pyrrolidone. *Langmuir* **2008**, *24*, 13742–13747.
- (30) Popescu, M.-T.; Tasis, D.; Tsitsilianis, C. Ionizable Star Copolymer-Assisted Graphene Phase Transfer between Immiscible Liquids: Organic Solvent/Water/Ionic Liquid. ACS Macro Lett. 2014, 3, 981–984.
- (31) Popescu, M.-T.; Tasis, D.; Papadimitriou, K. D.; Gkermpoura, S.; Galiotis, C.; Tsitsilianis, C. Colloidal stabilization of graphene sheets by ionizable amphiphilic block copolymers in various media. *RSC Adv.* **2015**, *5*, 89447–89460.
- (32) Han, C.; Guo, Y.; Chen, X.; Yao, M.; Zhang, Y.; Zhang, Q.; Wei, X. Phase behaviour and temperature-responsive properties of a gemini surfactant/Brij-30/water system. *Soft Matter* **2017**, *13*, 1171–1181.
- (33) Krieger, I. M.; Dougherty, T. J. A Mechanism for Non-Newtonian Flow in Suspensions of Rigid Spheres. *Trans. Soc. Rheol.* **1959**, 3, 137–152.
- (34) Krieger, I. M. Rheology of monodisperse latices. *Adv. Colloid Interface Sci.* **1972**, *3*, 111–136.
- (35) Vlassopoulos, D.; Fytas, G.; Pispas, S.; Hadjichristidis, N. Spherical polymeric brushes viewed as soft colloidal particles: zero-shear viscosity. *Phys. B* **2001**, 296, 184–189.
- (36) High Solid Dispersions; Cloitre, M., Ed.; Advances in Polymer Science; Springer: Berlin, Heidelberg, 2010; Vol. 236.
- (37) Bullard, J. W.; Pauli, A. T.; Garboczi, E. J.; Martys, N. S. A comparison of viscosity—concentration relationships for emulsions. *J. Colloid Interface Sci.* **2009**, 330, 186–193.
- (38) Bicerano, J.; Douglas, J. F.; Brune, D. A. Model for the Viscosity of Particle Dispersions. *J. Macromol. Sci. C Polym. Rev.* **1999**, 39, 561–642.
- (39) Shikata, T.; Pearson, D. S. Viscoelastic behavior of concentrated spherical suspensions. *J. Rheol.* **1994**, *38*, 601–616.
- (40) Mewis, J.; Wagner, N. Colloidal Suspension Rheology; Cambridge University Press, 2012.
- (41) Pal, R. Novel viscosity equations for emulsions of two immiscible liquids. *J. Rheol.* **2001**, *45*, 509–520.